EasyChair Preprint

№ 10968

Perturbation Observer-Based Feedback Linearization Control of Robotic Arm Platform

Zahra Ahangari Sisi, Mehdi Mirzaei, Sadra Rafatnia, Mohammad Mohammadi Shahir and Faezeh Pak

September 26, 2023

Perturbation Observer-based Feedback Linearization Control of Robotic Arm Platform

Zahra Ahangari Sisi
Faculty of Mechanical Engineering
Sahannd University of Technology
Tabriz, Iran.
z_ahangari98@sut.ac.ir

Mehdi Mirzaei
Faculty of Mechanical Engineering
Sahannd University of Technology
Tabriz, Iran.
mirzaei@sut.ac.ir

Sadra Rafatnia
Faculty of Mechanical Engineering
Sahannd University of Technology
Tabriz, Iran.
sa_rafatnia@sut.ac.ir

Mohammad Mohammadi Shahir
Faculty of Mechanical Engineering
Sahannd University of Technology
Tabriz, Iran.
mi.shahir74@gmail.com

Faezeh Pak
Faculty of Mechanical Engineering
Sahannd University of Technology
Tabriz, Iran.
f_pak99@sut.ac.ir

***Abstract*— This study aims to experimentally control of robotic arm position in the presence of model uncertainties and external disturbances. A feedback linearization controller (FLC) is designed based on a precise dynamic model, in which the perturbations are estimated using an extended state observer (ESO). The ESO employs the angular displacement of the arm as a measurable output, and adds the terms containing perturbations to the system equations as new state variables. By estimating the system states, an accurate model is provided to design the feedback linearization controller for tracking the desired paths of the arm. The stability analyses are presented, indicating the estimation and tracking errors are bounded. Finally, an experimental implementation on a fabricated platform of a robotic arm is given to illustrate the superior performance of the proposed control scheme.**

Keywords—Robot arm, Extended state observer, Feedback linearization controller, Perturbation rejection, Experimental implementation.

I. INTRODUCTION

Nowadays, robotic manipulators/arms are highlighted due to many advantages such as low cost, high accuracy, high load ratio, and decreased power consumption [1]. These devises are usually replacing human workers to help them with complicated and duplicate tasks such as transportation, handling, packing, coloring, welding, etc. [2]. To track the desired trajectories more closely, robotic manipulators are required to be precisely controlled. The important issue in the design of controllers is access to a reliable and precise model of the system and environmental conditions. The presence of the uncertainties, external disturbances and other perturbations are inevitable, affecting the accuracy of the model and consequently the performance of the designed control system. Estimation of these perturbations and updating of the system model is a suitable approach to achieve a reliable model for the controller design [3].

In the literature, extensive efforts have been made to control robot manipulators/arms in the presence of uncertainties and external disturbances to track the desired trajectory. Rojko et al. [4] proposed an adaptive fuzzy estimator for disturbance estimation in the direct-drive robot. Soltanpour et al. [5] developed a new approach of controller design using the sliding mode controller with the support of FLC and the backstepping method. Perrusquía [6] proposed a robust FLC for a direct-drive robot manipulator. In refs. [7,8], researchers developed a nonlinear optimal control system based on a predictive approach for trajectory tracking problem. Nikdel et al. [9] proposed an adaptive backstepping control method to control robotic manipulators and uncertainty estimation. Fateh et al. [10] applied an adaptive fuzzy controller to handle the robotics manipulator. Chang et al. [11] proposed an adaptive fuzzy backstepping control. In the reviewed studies, the researchers have usually focused on adaptive and robust control methods to cope with model uncertainties and external disturbances.

On the other hand, estimation methods are extended to compensate for uncertainties and external disturbances with no need to the extra control input. Agarwal et al. [12] presented a new observer that produced a new state to estimate disturbance, and then the EKF was applied to remove the noise in the disturbance estimation. Mohammadi Asl et al. [13] presented an adaptive extended Kalman filter for position estimation of the robotic manipulators utilized in a non-singular fast terminal sliding mode controller. The Kalman filter (KF) provides optimal solutions in noisy environments but needs information about the statistical characteristics of measurement uncertainties. Also, researchers are faced with adjusting the covariance matrices in the KF-based algorithms as a challenge. As another approach, the extended state observer (ESO) is presented to estimate uncertainties. In this method, model uncertainties are considered as extra state variables. Talole et al. [14] designed an ESO for states and uncertainties estimation and used the estimated states in a FLC. Yang et al. [15] proposed an ESO observer to estimate the nonlinearities of a two-link flexible manipulator based on a backstepping controller to track the trajectories. In [16], a dual extended state observer based on a dynamic surface controller is proposed for a manipulator with a hydraulic actuator. The ESO is an important approach to disturbance rejection, that is not dependent on specific mathematical models of disturbances [17].

This study deals with the design and experimentally implementation of an ESO-based FLC to overcome the uncertainties and external disturbances in the lever arm. The ESO utilizes the angular displacement of the lever arm measured by a 2-phase encoder. After estimating the model perturbations, the FLC is developed based on an updated model for tracking the desired path of the arm actuated by a

DC motor. The stability of the observer and controller is analyzed mathematically. The performance of the designed control system is evaluated experimentally for different trajectories with and without the observer. The results of FLC and ESO-based FLC are compared.

The paper is organized as follows: After Introduction, in the section 2, the overview of the kinetic model of the lever arm is presented. In the section 3, an ESO algorithm is developed. In the section 4, the controller is presented by the FLC. The results of the practical implementation are discussed in section 5. Finally, the conclusion is given in the last section.

II. Problem Statement

A schematic of lever arm is presented in Fig. 1. It consists of a massless arm with two lumped masses positioned at the end-points.

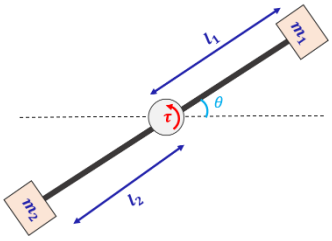

Fig 1. The schematic of the lever arm.

In order to derive the governing equations of the system, we adopt the Lagrange approach. In this respect, the kinematic and potential energies are derived as follow:

$$T = \frac{1}{2} I_o \dot{\theta}^2, \tag{1}$$

$$V_g = (m_1 l_1 - m_2 l_2)\, g\, sin\theta, \tag{2}$$

where I_o is the moment of inertia. m_1 and m_2 denote the end-point masses. θ is the angular displacements of the arm. The Lagrange equation for the lever arm is presented as

$$\frac{d}{dt}\left(\frac{\partial T}{\partial \dot{\theta}}\right) - \frac{\partial T}{\partial \theta} + \frac{\partial V_g}{\partial \theta} = \tau, \tag{3}$$

Consequently, the dynamics of the lever arm can be expressed as

$$I_o \ddot{\theta} + G(\theta) = \tau, \tag{4}$$

where $I_0 = m_1 l_1^2 + m_2 l_2^2$ denotes the inertia of the lever arm and $G = (m_1 l_1 - m_2 l_2) g \cos\theta$ is the gravity term. τ is the motor torque. By considering $\theta = x_1$. $\dot{\theta} = x_2$, the state-space model of the lever arm is represented as

$$\begin{cases} \dot{x}_1 = x_2, \\ \dot{x}_2 = -I_o^{-1} G(x_1) + I_o^{-1} u + d, \end{cases} \tag{5}$$

where u is the control input and $y \in R$ is the output of the manipulator. In practical scenarios, uncertainties and external disturbances within the lever arm model are unavoidable. These factors render the nominal model unsuitable for accurate simulation and controller design under real-world conditions. In this study, external disturbances are considered as follows:

$$d = 0.2 \sin(0.5t), \tag{6}$$

where $t \in [0, t_f]$ demonstrates the time index.

III. Extended State Observer Algorithm

In order to design a reliable model-based controller, an ESO is employed to estimate model perturbations of the system. Perturbations may include as unknown parameters, un-modeled dynamics, and external disturbances. A term encompassing modeling perturbations is considered an additional state, represented as $x_3 = f(x) = -I_o^{-1} G(x_1) + d$. Therefore, the state-space model of the lever arm is rewritten as

$$\begin{cases} \dot{x}_1 = x_2, \\ \dot{x}_2 = f(x) + I_o^{-1} u, \\ \dot{x}_3 = \gamma(t), \end{cases} \tag{7}$$

where $\gamma(t) = \dot{f}(x)$ is assumed to be an unknown but bounded function. By considering $y = x_1$ as the system output, the steady state observer of Eq. (7) is manufactured as

$$\begin{cases} \dot{z}_1 = z_2 + \beta_1 (x_1 - z_1), \\ \dot{z}_2 = z_3 + I_o^{-1} u + \beta_2 (x_1 - z_1), \\ \dot{z}_3 = \beta_3 (x_1 - z_1), \end{cases} \tag{8}$$

where $\beta_i (i = 1,2,3)$ are the observer gains.

By merging equations (7) and (8), we can formulate the equations for observer errors as follow:

$$\begin{cases} \dot{\tilde{z}}_1 = \tilde{z}_2 - \beta_1 \tilde{z}_1, \\ \dot{\tilde{z}}_2 = \tilde{z}_3 - \beta_2 \tilde{z}_1, \\ \dot{\tilde{z}}_3 = \gamma(t) - \beta_3 \tilde{z}_1, \end{cases} \tag{9}$$

where $\tilde{z}_i = x_i - z_i, i = 1,2,3$ shows the observer error. By selecting suitable values for observer gains, we can guarantee the input-output stability of the observer while also considering the bounded nature of γ.

Theorem 1. By selecting $\beta_1 = 3/\epsilon$, $\beta_2 = 3/\epsilon^2$, and $\beta_3 = 1/\epsilon^3$, in which ε is a positive free parameter, the estimation error dynamic (9) is bounded under the assumption that $\gamma(t)$ is bounded.

Proof. Using $\beta_1 = 3/\epsilon$, $\beta_2 = 3/\epsilon^2$, and $\beta_3 = 1/\epsilon^3$, in the estimation error dynamic (9) leads to

$$\begin{bmatrix} \dot{\tilde{z}}_1 \\ \dot{\tilde{z}}_2 \\ \dot{\tilde{z}}_3 \end{bmatrix} = A \begin{bmatrix} \tilde{z}_1 \\ \tilde{z}_2 \\ \tilde{z}_3 \end{bmatrix} + B\gamma(t). \tag{10}$$

where $A = \begin{bmatrix} -3/\epsilon & 1 & 0 \\ -3/\epsilon^2 & 0 & 1 \\ -1/\epsilon^3 & 0 & 0 \end{bmatrix}$ and $B = \begin{bmatrix} 0 \\ 0 \\ 1 \end{bmatrix}$. The characteristic polynomial of A is $\lambda = s^3 + \frac{3}{\epsilon} s^2 + \frac{3}{\epsilon^2} s + \frac{1}{\epsilon^3} = \left(s + \frac{1}{\epsilon}\right)^3$ which indicates that the eigenvalues of A are equal to $s_i = -\frac{1}{\epsilon}$ $(i = 1,2,3)$. Therefore, for a given $\epsilon > 0$, the matrix A is Hurwitz and ε affects the convergence speed of the observer. The first order differential equation of (10) is solved as

$$\tilde{z}(t) = e^{At} \tilde{z}(0) + \int_0^{t_f} e^{A(t_f - \vartheta)} B\gamma(\vartheta) d\vartheta, \tag{11}$$

It is clear, for smaller positive values of ϵ, the system response will be faster and the steady-state estimation error converges to

$$\lim_{t \to \infty} \tilde{z}(t) = \int_0^t e^{A(t-\vartheta)} B\gamma(\vartheta) d\vartheta. \tag{12}$$

It is concluded from (12), by considering boundedness of $\gamma(\vartheta)$, estimation error will be bounded ■

Remark. The free parameter ϵ influences the placement of the eigenvalues and consequently the speed of the ESO as a high-gain observer. For larger values of ϵ, the response

speed decreases, and for smaller values of free parameter ϵ, despite faster responses, the system becomes sensitive to measurement noise and modeling errors, leading to fluctuations with high frequency. Furthermore, numerical errors may occur when solving the set of differential equations at each sampling time [18].

IV. ESO-BASED FEEDBACK LINEARIZATION CONTROLLER

The overall structure of the proposed control method is shown in Fig. 2. By using angular displacement measurement and the control input, the system states are estimated by the ESO observer. The proposed estimation algorithm not only aims to estimate the state variables, but also strives to minimize the discrepancy between the initial model and the actual model. Therefore, by assuming access to accurate dynamics of the system, a controller with the structure of feedback linearization is firstly designed based on the model described by (5). Then, the supervisor updates the initially designed model after receiving information from the observer and then utilizes the updated model including all model uncertainties to develop an ESO-based FLC for tracking the desired trajectory.

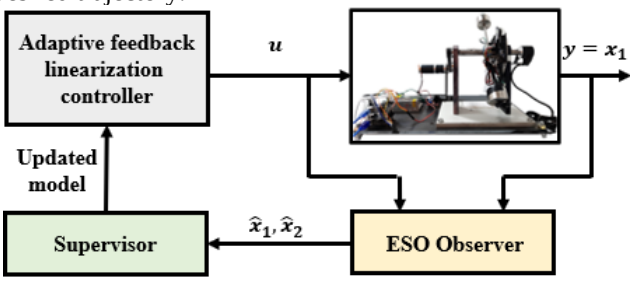

Fig 2. The overall structure of the proposed control method.

According to Eq. (5), the system has the relative degree $\rho = 2$ since the control signal u first appears in the second derivative of x_1 as follow

$$\ddot{y} = -I_o^{-1}G(x_1) + I_o^{-1}u + d. \tag{13}$$

The feedback linearization control law is derived in the presence of uncertainties and with access to precise dynamics as follows

$$u = -I_o(\beta - \alpha), \tag{14}$$

where

$$\beta = -I_0^{-1}G(x_1) + d, \tag{15}$$

will be available by the ESO. Considering $\alpha = \ddot{x}_{1d} - k_1(x_2 - \dot{x}_{1d}) - k_2(x_1 - x_{1d})$, the error dynamics can be written as

$$\ddot{e} + k_1\dot{e} + k_2 e = \kappa, \tag{17}$$

where $e = x_1 - x_{1d}$. According to Theorem. 1, the ESO is a bounded-input bounded-output observer and the estimation error are considered as the term κ in the right-hand side of error dynamic (17). Therefore, the following theorem is presented to demonstrate the stability of the proposed control method in the presence of bounded estimation errors of uncertainties, and disturbances.

Theorem 2. The tracking error of the proposed controller (14) will be bounded in the presence of bounded estimation errors of uncertainties and disturbances. Also, to converge the tracking error to the compact set, the poles of the controller should be selected far away from the imaginary axis.

Proof. By considering the upper bound for the estimation error as $|\kappa| < \mu$, Eq. (17) is rewritten as

$$\ddot{e} + k_1\dot{e} + k_2 e \le \mu. \tag{18}$$

Solving the second-order differential inequality (18) and utilizing the comparison lemma [19] leads to

$$e \le \begin{cases} c_1 e^{-\frac{1}{2}(k_1+\sqrt{\Delta})} + c_2 e^{-\frac{1}{2}(k_1-\sqrt{\Delta})} + \frac{\mu}{k_2} & \text{if} \quad \Delta > 0, \\ e^{-\frac{1}{2}k_1 t}\,(c_3 + c_4 t) + \frac{\mu}{k_2} & \text{if} \quad \Delta = 0, \\ c_5 e^{-\frac{1}{2}k_1 t}\, sin(\frac{\sqrt{\Delta}}{2}t + \varphi) + \frac{\mu}{k_2} & \text{if} \quad \Delta < 0, \end{cases} \tag{19}$$

where $\Delta = k_1^2 - 4k_2$ and $c_{i\ (i=1,\dots,5)}$ are constant values. Considering positive values for k_1 and k_2, all three cases above, leads to

$$\lim_{t\to\infty} e(t) = \frac{\mu}{k_2}. \tag{20}$$

Based on Eq. (20), for a given $\sigma > 0$, the coefficient k_2 can be selected as $\frac{\mu}{\sigma} < k_2$ so that the tracking error can converge within the following compact set:

$$|e| < \sigma. \tag{21}$$

To analysis the boundedness of $\dot{e}$, the following candidate Lyapunov function is defined:

$$V = \frac{k_2}{2}e^2 + \frac{1}{2}\dot{e}^2 > 0. \tag{22}$$

Derivation from Eq. (22) gives

$$\dot{V} = k_1 e\dot{e} + \dot{e}\ddot{e}. \tag{23}$$

By substituting Eq. (17) into Eq. (23), and considering the upper bound $|\kappa| < \mu$, the following inequality can be derived:

$$\dot{V} \le -k_1\dot{e}^2 + \mu|\dot{e}|. \tag{24}$$

By applying the inequality $ab \le na^2 + \frac{b^2}{4n}$ for any real a, b, and $n > 0$ to the last terms of inequality (24) and supposing $n = \frac{1}{k_1}$, Eq. (24) is rewritten as

$$\dot{V} \le -\frac{3}{4}k_1\dot{e}^2 + \frac{\mu^2}{k_1}. \tag{25}$$

By using (21) and (22), inequality (25) can be rewritten as

$$\dot{V} \le -\frac{3}{2}k_1 V + \frac{3}{4}k_1 k_2\sigma^2 + \frac{\mu^2}{k_1}. \tag{26}$$

By taking $\frac{3}{4}k_1k_2\sigma^2 + \frac{\mu^2}{k_1} = \emptyset$, inequality (26) is rewritten as

$$\dot{V} \le -\frac{3}{2}k_1 V + \emptyset. \tag{27}$$

Solving Eq. (27) via the comparison lemma leads to

$$V \le (V(0) - \frac{\emptyset}{k_1})e^{-k_1 t} + \frac{\emptyset}{k_1}. \tag{28}$$

If k_1 is a positive value, the Lyapunov function will be bounded as:

$$\lim_{t\to\infty} V(t) = \frac{\emptyset}{k_1}. \tag{29}$$

Since the Lyapunov function defined by (29) is bounded, and also the tracking error is within the compact set according to (21), so $\dot{e}$ will be bounded.

V. RESULTS AND DISCUSION

In this section, a fabricated platform for a robotic arm is utilized to evaluate the performance of the proposed method. In the proposed method, uncertainties and disturbances are treated as an extended state, and the link position information

is used to estimate this state in conjunction with the angular velocity of the link states. The control system designed based on the proposed observer can adapt itself to real-world conditions and utilize sufficient information about uncertainties and disturbances. In addition to the unmodeled dynamics and disturbances presented in Eq. (6), we also consider a 10% parametric uncertainty in the inertia of the lever arm.

The test equipment is shown in Fig. 3. According to this figure, the HN3806 two-phase encoder measures the angular displacement of the arm with an accuracy of 0.05 (Deg) at the 50 Hz frequency. After measuring the sensor output, the control signal is calculated, and the pulse width modulation (PWM) of the motor is sent to the motor driver. Finally, a 12-volt DC motor produces the proposed control input. To validate the proposed controller, the MATLAB-Simulink environment is used to read the sensors outputs, to calculate the control input and to send the control signals to the actuator. The platform setup parameters are presented in Table I.

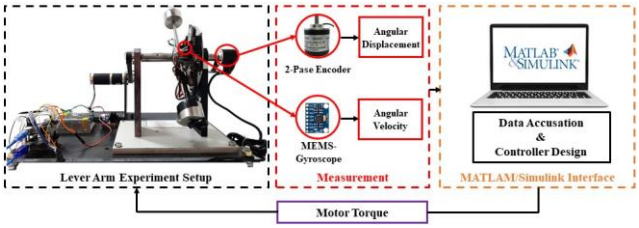

Fig. 3. Fabricated platform of the lever arm.

TABLE I. PARAMETERS OF THE FABRICATED PLATFORM

Parameter	Discreption	Value
m_1	lumped mass 1	0.5 kg
m_2	lumped mass 2	0.55 kg
l_1	Length of arm 1	0.15 m
l_2	Length of arm 2	0.14 m
I_o	moment of inertia	0.0225 kg.m^2

At the first test called test-1, the performance of the ESO-based FLC is evaluated for different values of ϵ. Figure 4(a) illustrates that when the value of the free parameter is set to $\epsilon = 0.09$, the ESO can accurately estimate the perturbations, and the proposed control method provides significant performance in tracking the desired path. For larger values of ϵ, the robotic arm dynamics cannot be accurately captured and the estimation errors are increased. On the other hand, for smaller values of free parameters like $\epsilon = 0.05$, despite faster responses, the system becomes sensitive to measurement noise and thus modeling errors, leading to fluctuations with high frequency and numerical errors. The control inputs related to the three different ϵ are shown in Fig. 4(c). The results reveal that the value of the free parameter ϵ should not be selected too large or too small to prevent large errors and high fluctuations in the responses and control inputs. It is concluded from the results that, a suitable value $\epsilon = 0.09$ is selected for the present application. To compare the performance of the proposed approach for different values of ϵ, the root mean square (RMS) of tracking errors and control inputs are reported in Table II. When $\epsilon = 0.09$, the RMS of tracking error and control input is the lowest in comparison with smaller and bigger values of ϵ

Figure 5 shows a comparison between the estimation of the angular velocity and unknown term ($\hat{x}_3$) for three free parameters of ϵ. The superior accuracy of the proposed controller for $\epsilon = 0.09$ in comparison to another magnitudes is clearly seen.

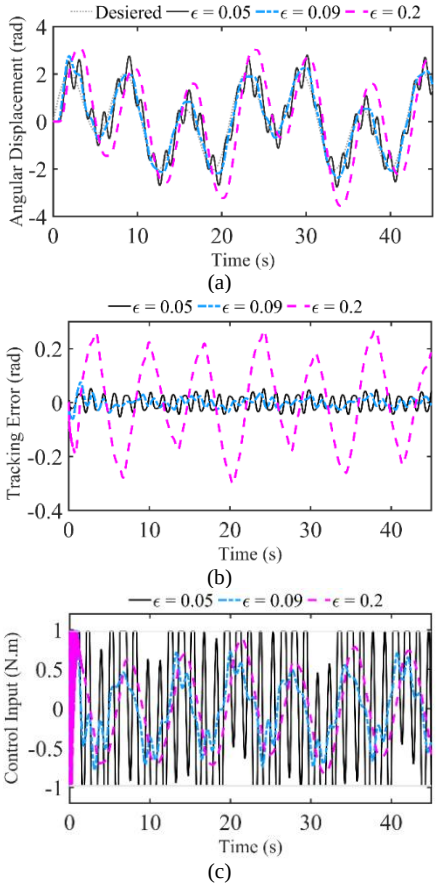

Fig. 4. The experimental results of the ESO-based FLC in test-1 for different values of ϵ. (a) Angular displacement, (b) Tracking error, (c) Control input.

TABLE II. THE RMS OF THE RESPONCES FOR DIFFERENT VALUES OF FREE PARAMETER IN TEST-1.

Different values of ϵ	$\epsilon = 0.05$	$\epsilon = 0.09$	$\epsilon = 0.2$
Tracking error (rad)	0.0259	0.0182	0.1582
Control input (N.m)	0.8096	0.4141	0.5135

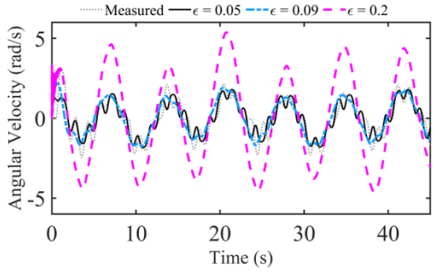

(a)

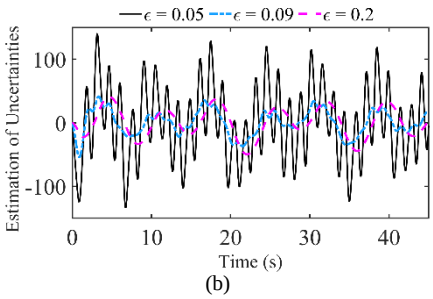

(b)

Fig. 5. The experimental results in test-1 for different values of ϵ (a) Angular velocity, (b) Estimation of unknown term.

In order to verified the proposed controller in different conditions, a time-varying reference trajectory is considered as test-2. The result of the proposed controller for different value of ϵ is shown in Fig. 6. Also, the RMS of the tracking errors and control inputs are reported in Table III. The results indicate the high efficiency of the proposed method for $\epsilon = 0.09$.

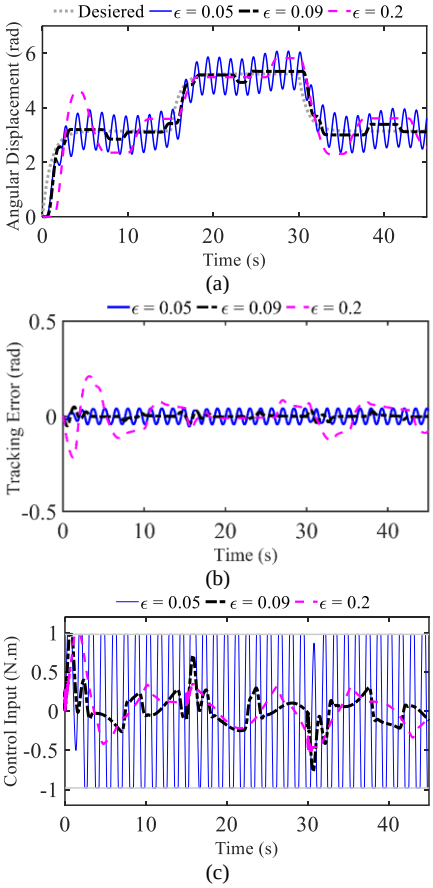

(c)

Fig. 6. The experimental results of the ESO-based FLC in test-2 for different values of ϵ (a) Angular displacement, (b) Tracking error, (c) Control input.

TABLE III. THE RMS OF THE RESPONCES FOR DIFFERENT VALUES OF FREE PARAMETER IN TEST-2.

Different values of ϵ	$\epsilon = 0.05$	$\epsilon = 0.09$	$\epsilon = 0.2$
Tracking error (rad)	0.0294	0.0119	0.0751
Control input (N.m)	0.8563	0.2244	0.2733

Fig. 7 shows the effect of uncertainties estimation in the performance of the controller. When the uncertainties are not estimated, the controller design is based on the initial model of the system without updating. As demonstrated in Fig. 7, controller with uncertainty estimation is much better than the controller without uncertainty estimation. This is for the reason that the observer attempts to enhance the reliability of the initial model by adding the uncertainty term. Therefore, the controller that uses the updated model has a good performance in decreasing the tracking error.

CONCLUSION

In this paper, the perturbation of a robotic arm is considered as an additional state and estimated by extended state observer. Accordingly, a feedback linearization controller based on the updated model is designed for the trajectory tracking of a robotic manipulator. Different tests under various dynamical maneuvering are conducted to show the performance of the proposed algorithm. The experimental result indicates the efficiency of the proposed control method in reducing the tracking error in the presence of various sources of uncertainties and disturbances.

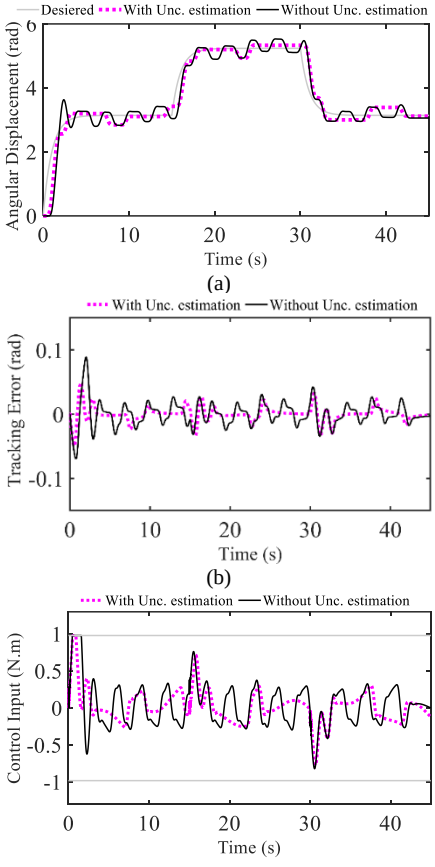

(c)

Fig. 7. The experimental results of the ESO-based FLC in test-2 with and without uncertainties estimation. (a) Angular displacement, (b) Tracking error, (c) Control input.

REFERENCES

[1] B. Hazrat, B. Yin, M.Sh. Aslam, Z. Anjum, A. Rohra, and Y. Wang, "A practical study of active disturbance rejection control for rotary flexible joint robot manipulator,"Soft Computing 27, no. 8, pp.4987-5001, 2023.

[2] B. Jaemin, and M. Kang. "A practical adaptive sliding-mode control for extended trajectory-tracking of articulated robot manipulators," IEEE Access,10, pp.116907-116918, 2022.

[3] H. Razmjooei, M. H. Shafiei. "A new approach to design a finite-time extended state observer: uncertain robotic manipulators application," International Journal of Robust and Nonlinear Control, 31(4), pp.1288-1302, 2021.

[4] R. Andreja, and K. Jezernik. "Sliding-mode motion controller with adaptive fuzzy disturbance estimation," IEEE Transactions on Industrial Electronics,51(5), pp.963-971, 2004.

[5] M. R., Soltanpour, and M. M. Fateh. "Sliding mode robust control of robot manipulators in the task space by support of feedback linearization and backstepping control," World Applied Sciences Journal, 6(1), pp.70-76, 2009.

[6] A. Perrusquía, "Robust state/output feedback linearization of direct drive robot manipulators: A controllability and observability analysis," European Journal of Control, 64, p.100612, 2022.

[7] N. Ahmadlou, M. Mirzaei, S. Rafatnia, "Design of a constrained controller for wheeled mobile robot implemented in V-Rep simulator," In 2021 9th RSI International Conference on Robotics and Mechatronics (ICRoM), pp. 491-496.

[8] S. K. Samiei, M. Mirzaei, N. Yarinia, S. Rafatnia, "Design and practical implementation of an input-constrained nonlinear controller for a single-link flexible joint robotic manipulator," In 2022 10th RSI International Conference on Robotics and Mechatronics (ICRoM), pp. 551-556

[9] N. Nikdel, M. Badamchizadeh, V. Azimirad, M. A. Nazari, "Fractional-order adaptive backstepping control of robotic manipulators in the presence of model uncertainties and external disturbances," IEEE Transactions on Industrial Electronics, 63(10), pp.6249-6256, 2016.

[10] S. Fateh, M. M. Fateh, M. M., "Adaptive fuzzy control of robot manipulators with asymptotic tracking," Journal of Control, Automation and Electrical Systems, 31, pp.52-61, 2020.

[11] W. Chang, Y. Li, S. Tong, "Adaptive fuzzy backstepping tracking control for flexible robotic manipulator," IEEE/CAA Journal of Automatica Sinica, 8(12), pp.1923-1930, 2018.

[12] V. Agarwal, H. Parthasarathy, "Disturbance estimator as a state observer with extended Kalman filter for robotic manipulator," Nonlinear Dynamics, 85, pp.2809-2825,2016.

[13] R. M. Asl, Y. S. Hagh, H. Handroos, H, "Adaptive extended Kalman filter designing based on non-singular fast terminal sliding mode control for robotic manipulators," In 2017 IEEE International Conference on Mechatronics and Automation (ICMA). pp. 1670-1675.

[14] S. E., Talole, S. E. Phadke, "Extended state observer based control of flexible joint system," In 2008 IEEE International Symposium on Industrial Electronics, pp. 2514-2519.

[15] H. Yang, Y. Yu, Y. Yuan, X. Fan, "Back-stepping control of two-link flexible manipulator based on an extended state observer," Advances in space research, 56(10), pp. 2312-2322, 2015.

[16] X. Zhang, D. Shi, G, "Dual extended state observer-based adaptive dynamic surface control for a hydraulic manipulator with actuator dynamics," Mechanism and Machine Theory, 169, p.104647, 2022.

[17] J. Han, "From PID to active disturbance rejection control," IEEE transactions on Industrial Electronics, 56(3), pp.900-906, 2009.

[18] S. Rafatnia, M. Mirzaei, "Adaptive estimation of vehicle velocity from updated dynamic model for control of anti-lock braking system," IEEE Transactions on Intelligent Transportation Systems, 23(6), pp.5871-5880, 2021.

[19] HK. Khalil, "Nonlinear Control: Adaptation and Learning," Singapore: World Scientific, 2015.